Pan-Cancer Analysis of VIM Expression in Human Cancer Tissues

Małgorzata Blatkiewicz (blatkiewicz.malgorzata@gmail.com)
University of Szczecin: Uniwersytet Szczecinski https://orcid.org/0000-0001-5506-2397
Piotr Białas
Poznan University of Medical Sciences: Uniwersytet Medyczny imienia Karola Marcinkowskiego w Poznaniu
Olga Taryma-Leśniak
Pomeranian Medical University in Szczecin: Pomorski Uniwersytet Medyczny w Szczecinie
Beata Hukowska-Szematowicz
University of Szczecin: Uniwersytet Szczecinski

Research article

Keywords: vimentin, TCGA, STRING, expression, methylation, cancer

Posted Date: June 23rd, 2021

DOI: https://doi.org/10.21203/rs.3.rs-646169/v1

Abstract

In 2020, more than 19 million cancer cases were diagnosed. One of the best paths to more effective treatment with a chance of being cured for patients is early detection. Vimentin (VIM), as an intermediate filament protein, is broadly expressed in mesenchymal cells. VIM is responsible for several biological processes such as cellular component organization and biogenesis, metabolic processes, and biological regulation. A growing body of literature indicates that expression of the VIM gene (*VIM*) is disrupted in carcinomas during epithelial–mesenchymal transition. Herein, we broadly analyzed the gene expression and promoter methylation profile of *VIM* in 19 cancer types across The Cancer Genome Atlas (TCGA). Furthermore, the protein–protein interactions (GeneMANIA and Search Tool for the Retrieval of Interacting Genes (STRING) database) and the alteration frequency of mutations (cBioPortal database) in *VIM* were analyzed. We proved that *VIM* is overexpressed in seven of the 19 studied cancer types. For two of them, we observed an association of *VIM* expression with gene promoter methylation. It must be emphasized that *VIM* overexpression can be a potential diagnostic biomarker in selected types of cancers.

1. Introduction

The vimentin gene (*VIM*) is a single-copy gene, located on the short arm of chromosome 10 (10p12) (Rittling and Baserga 1987). The *VIM* promoter is composed of three different elements which regulate the gene expression. *VIM* codes for a 57 kDa polypeptide, vimentin, which is one of the most widely expressed and highly conserved proteins of the type III intermediate filament (IF) protein family. The primary biological function of vimentin is to maintain cellular integrity and provide resistance to cellular stress. Moreover, vimentin may form a complex with cell **signaling** molecules and other adaptor proteins (Eriksson 2009). The cellular localization of vimentin is directly related to its function. The protein forms networks around the cell nucleus and extends from there to the entire cytoplasm, creating a scaffold for cell organelles (Franke 1978; Lowery 2015). The *VIM* product is a multifunctional protein that can also interact with several other proteins, making it a potential regulator of several physiological processes. In recent years, there has been growing evidence that, during pathological condition such as tissue injury, inflammation, or cancers, vimentin could also be localized outside the cell (Yu 2018). These findings demonstrate that *VIM* may be a potential diagnostic biomarker not only in cancer, but also in autoimmune disorders (e.g., Crohn's disease), viral infections (e.g., human immunodeficiency virus (HIV)), and severe acute respiratory syndrome coronavirus 2 (SARS-CoV-2) (Fernandez-Ortega 2016; Yu 2016; Li and Kuemmerle 2020; Li 2020; Zhang 2020; Suprewicz 2021). As an IF protein, vimentin is expressed in many different cells and tissues with a diverse expression abundance. The data from the Human Protein Atlas (https://www.proteinatlas.org/) show that human tissues, such as the ovaries, breasts, lungs, and bone marrow, are characterized by increased *VIM* expression (Uhlen 2015), while limited expression of *VIM* is observed in the stomach, rectum, and liver tissue (Uhlen 2015). Within human immune cells, an increased level of *VIM* was shown in activated macrophages, in contrast to a limited level of expression in T and B lymphocytes, and a lack of expression in Burkitt's lymphoma cell lines (Cain 1983; Perreau 1988; Sommers 1989). Moreover, it has been observed that *VIM* is expressed in many hormone-independent mammary carcinoma cell lines (Perreau 1988; Sommers 1989).

Current epidemiological data from reports of the World Health Organization (WHO), the International Agency for Research on Cancer (IARC), and the Union for International Cancer Control (UICC) indicate that, over the next two decades, cancer will be the leading cause of death. Cancer diseases are related to unrestrained cell growth which can spread to other parts of the body. Cancer cell invasiveness is, in fact, a key feature of metastatic tumors enabling them to (i) break away from the tumor (separation), (ii) invade through local tissue (invasion), (iii) infiltrate blood (and lymph) vessels (intravasation), (iv) circulate in the blood stream (survival), (v) exit from circulation (extravasation), and (vi) take up residence in vital organs (arrest). Aggressive tumors often metastasize locally or distantly to other organs, causing significant morbidity and mortality (Loberg 2005; Siegel 2021). Accordingly, 19,292,789 cases of all cancers were reported in 2020 (Siegel 2021). The five most common types of cancer according to the World Health Organization are breast, lung, colorectal, prostate, and stomach cancer (Fig. 1). As a function of gender, the most often diagnosed are breast, lung, and colorectal cancer in women, and lung, prostate, and colorectal cancer in men (according to the Globocan data source, International Agency for Research on Cancer, World Health Organization, https://gco.iarc.fr/today/home).

A growing body of literature indicates that vimentin controls cell proliferation (Cheng 2016). Extensive research in vimentin-deficient animal models (for example, *vim*$^{-/-}$ mice) showed that loss of vimentin caused a reduction in fibrosis and the mesenchymal phenotype of cells (for example, in cholangiocytes), which could be reversed upon *vim* re-expression (Eckes 1998; Zhou 2019). In contrast, some oncogenes could increase cell proliferation, as a result of a higher vimentin messenger RNA (mRNA) and protein

levels (Rathje 2014). Furthermore, *VIM* expression could be stimulated by lipopolysaccharides (LPS) in the Jurkat cell line and promote apoptosis (Lee 2014). These findings lead us to suspect that overexpression of *VIM* could be a key therapeutic target in particular cancers.

Evaluation of *VIM* expression patterns in normal and cancer tissues can be of considerable value in tumor diagnosis and progression. In the present study, we comprehensively analyzed *VIM* expression, promoter methylation, and their association with cancer patients using The Cancer Genome Atlas (TCGA) UALCAN database. As previous studies reported a correlation between *VIM* expression and gene promoter methylation level in different cancer types, such as breast cancer (Ulirsch 2013), colorectal cancer (Li 2018), and gastric cancer (Cong 2016), here in we analyzed whether overexpression of *VIM* in the cancer types defined in our study is associated with gene promoter methylation. Additionally, to reveal the potential mechanism of *VIM* in cancers, we investigated the functional network of the *VIM* product using GeneMANIA and the protein–protein interaction using the Search Tool for the Retrieval of Interacting Genes (STRING) interactive online tool. These findings provide useful information about the correlation between *VIM* expression and cancer diseases.

2. Methods

2.1. Analysis of VIM mRNA Expression Levels in Distinct Types of Human Cancers Using UALCAN Web Portal

UALCAN is an interactive online web portal of genomics data from The Cancer Genome Atlas (TCGA) (http://ualcan.path.uab.edu/index.html) (Chandrashekar 2017). This user-friendly web platform performs analysis according to the level of gene expression of selected genes and compares them with clinical data from 33 cancer types.

The UALCAN web portal allows correlating the relative expression of selected genes across tumor and normal samples. Moreover, it provides data of patients' gender, age, body weight, race, and many other clinicopathological features such as patient survival or individual cancer stages. TCGA level 3 RNASeq V2 data corresponding to normal tissue and primary tumor samples are presented as a box-and-whisker plot generated by the website. For this work, all values of gene expression level are presented as transcripts per million (TPM), which is a normalization method for RNA sequencing (RNA-seq). The significant differences in gene expression between primary tumor (in clinical stages) and normal tissue were analyzed using online statistical analysis, whereby Student's *t*-test was used to calculate the level of statistical significance (*p*-value). The statistical significance of observed patterns is presented as *p*-values ($p \leq 0.05$). The data are presented using figures showing the interquartile range (IQR), the median, minimum, and maximum values, and the 25th (lower Q) and 75th (upper Q) percentiles.

2.2. Analysis of VIM Promoter Methylation Using UALCAN Web Portal

The UALCAN web portal was used to analyze differences in *VIM* promoter methylation level in normal tissue and primary tumor samples. The methylation level, ranging from 0 (unmethylated) to 1 (fully methylated) was estimated using the beta-value, which is the ratio of the methylated probe intensity to the sum of methylated and unmethylated probe intensity. The boxplot available on the UALCAN web portal represented the mean of beta-values from eight CpGs located up to 1500 bp upstream of the *VIM* transcription start site (TSS). The significant differences in promoter methylation level between normal tissue and primary tumor samples were analyzed using Student's *t*-test. The statistical significance of observed patterns is presented as *p*-values ($p \leq 0.05$).

2.3. Analysis of VIM Networks Using GeneMANIA and STRING Web Portal

The protein–protein networks of *VIM* were predicted using GeneMANIA analysis (http://www.genemania.org) (Warde-Farley 2010; Zuberi 2013). This online tool allows visualizing gene networks through bioinformatics methods, such as physical interaction, gene co-expression, gene co-localization, gene enrichment analysis, and website prediction. Functional protein partners for VIM were identifies using the Search Tool for the Retrieval of Interacting Genes (STRING) (version 11.0) analysis web portal (https://string-db.org/) (Szklarczyk 2019). The score of minimum required interaction was medium confidence (0.4).

2.4. Analysis of VIM Mutation Using cBioPortal

Analysis of *VIM* nonsynonymous mutations in cancer genomes was performed using the cBioPortal for Cancer Genomics (https://www.cbioportal.org/) online platform (Gao 2013). cBioPortal allows performing complex bioinformatics analyses and

generating graphical summaries of selected genes. The graphical presentation of mutation analysis constitutes colored plots indicating mutations, fusions, amplifications, deep deletions, and multiple alterations.

3. Results

3.1. VIM Expression Levels in Distinct Types of Human Cancers

According to TCGA UALCAN web-portal, a higher expression of *VIM* was found in seven from 19 cancers (Fig. 2).

Figure 2. Expression level of vimentin gene (*VIM*) in normal and cancer tissues, according to The Cancer Genome Atlas (TCGA). Blue box plots depict normal tissue, whereas red box plots depict primary tumor samples. TPM—transcripts per million; BLCA—bladder urothelial carcinoma; BRCA—breast invasive carcinoma; CESC—cervical squamous cell carcinoma; CHOL—cholangiocarcinoma; COAD—colon adenocarcinoma; ESCA—esophageal carcinoma; GBM—glioblastoma multiforme; HNSC—head-and-neck squamous cell carcinoma; KICH—kidney chromophobe; KIRC—kidney renal clear cell carcinoma; KIRP—kidney renal papillary cell carcinoma; LIHC—liver hepatocellular carcinoma; LUAD—lung adenocarcinoma; LUSC—lung squamous cell carcinoma; PAAD—pancreatic adenocarcinoma; PRAD—prostate adenocarcinoma; PCPG—pheochromocytoma and paraganglioma; READ—rectum adenocarcinoma; SARC—sarcoma; SKCM—skin cutaneous melanoma; THCA—thyroid carcinoma; THYM—thymoma; STAD—stomach adenocarcinoma; UCEC— uterine corpus endometrial carcinoma.

From TCGA database, we retrieved a dataset containing complete information on the *VIM* expression, gender, and promoter methylation of patients from 19 different types of cancers (Table 1).

Overexpression of *VIM* was found in cholangiocarcinoma (CHOL), glioblastoma multiforme (GBM), head-and-neck squamous cell carcinoma (HNSC), kidney renal clear cell carcinoma (KIRC) (Fig. 3A,C,E,G), kidney renal papillary cell carcinoma (KIRP), liver hepatocellular carcinoma (LIHC), and pheochromocytoma and paraganglioma (PCPG) (Fig. 4A,C,E). The analysis showed that the expression of *VIM* was significantly decreased in bladder urothelial carcinoma (BLCA), breast invasive carcinoma (BRCA), colon adenocarcinoma (COAD), lung adenocarcinoma (LUAD), lung squamous cell carcinoma (LUSC), and rectum adenocarcinoma (READ) (Fig. 5A,C,E,G,I,K). On the other hand, in esophageal carcinoma (ESCA), pancreatic adenocarcinoma (PAAD), sarcoma (SARC), stomach adenocarcinoma (STAD), thymoma (THYM), and thyroid carcinoma (THCA), there were no significant differences in the expression of *VIM* between cancer tissues and normal tissues.

Table 1

Expression level of *VIM* in normal and primary tumor tissues according to data deposited in TCGA database. A *p*-value ≤ 0.05 was considered statistically significant (bolded in table).

	Values of VIM expression in normal tissue				Values of VIM expression in primary tumor tissue				
Tumor type	Number of samples	Minimal value	Median	Maximal Value	Number of samples	Minimal value	Median	Maximal value	p-Value
BLCA	19	202.96	946.84	1868.49	408	18.08	243.59	1213.30	**1.92228×10^{-3}**
BRCA	114	349.75	2266.87	5778.52	1097	64.80	877.85	2388.66	**1.624478×10^{-12}**
CHOL	9	48.62	91.38	249.34	36	83.13	826.36	2131.32	**7.6293×10^{-4}**
COAD	41	210.71	434.87	878.06	286	30.2	245.46	932.01	**3.6207×10^{-4}**
ESCA	11	119.31	173.87	614.85	184	58.26	382.02	1323.80	6.9078×10^{-1}
GBM	5	289.62	315.13	377.42	156	707.82	3474.58	7278.70	**1.624478×10^{-12}**
HNSC	44	57.21	205.48	868.84	520	48.99	453.823	1633.74	**9.7606×10^{-5}**
KIRC	72	200.10	466.96	983.38	533	34.97	3433.38	6955.79	**1.624367×10^{-12}**
KIRP	32	279.41	452.62	922.6	290	75.8	1486.24	2948.53	**$< 1 \times 10^{-12}$**
LIHC	50	21.68	88.59	212.58	371	23.98	142.19	477.87	**1.161504×10^{-11}**
LUAD	59	935.59	1729.38	2705.30	515	66.07	725.15	1962.39	**$< 1 \times 10^{-12}$**
LUSC	52	1058.621	1929.41	3340.47	503	33.66	440.28	1601.93	**1.624478×10^{-12}**
PAAD	4	1105.65	1669.09	1973.93	178	26.79	984.38	2240.92	1.68864×10^{-1}
PCPG	3	473.25	477.67	482.08	179	28.02	553.12	1647.56	**2.1326×10^{-7}**
READ	10	243.24	561.82	807.12	166	36.64	247.13	723.83	**9.6001×10^{-4}**
SARC	2	475.66	850.43	1225.19	260	387.71	2603.49	7776.65	1.24304×10^{-1}
STAD	34	67.85	613.80	1575.87	415	51.06	529.51	1527.29	7.7998×10^{-1}
THCA	59	1281.31	2614.33	3797.93	505	455.75	2278.46	4620.76	4.946×10^{-1}
THYM	2	769.74	2080.50	3391.26	120	101.64	558.07	1537.33	5.2184×10^{-2}

BLCA—bladder urothelial carcinoma; BRCA—breast invasive carcinoma; CHOL—cholangiocarcinoma; COAD—colon adenocarcinoma; ESCA—esophageal carcinoma; GBM—glioblastoma multiforme; HNSC—head-and-neck squamous cell carcinoma; KIRC—kidney renal clear cell carcinoma; KIRP—kidney renal papillary cell carcinoma; LIHC—liver hepatocellular carcinoma; LUAD—lung adenocarcinoma; LUSC—lung squamous cell carcinoma; PAAD—pancreatic adenocarcinoma; PCPG—pheochromocytoma and paraganglioma; READ—rectum adenocarcinoma; SARC—sarcoma; STAD—stomach adenocarcinoma; THCA—thyroid carcinoma; THYM—thymoma.

It has to be noted that the analysis for BRCA ($n = 1097$) was performed on the highest number of primary tumor samples, in contrast to CHOL ($n = 36$), where the number of samples was the lowest. The highest median of the *VIM* transcript was found for GBM

(3474.583), and the poorest was found for LIHC (142.187) (Table 1).

To further investigate, we performed an analysis of *VIM* expression according to the clinicopathological features of selected cancers in the UALCAN database (Figs. 3–6). Analysis of *VIM* expression in cancer tissue as a function of gender only showed significant differences between male and female in BRCA, GBM, KIRC, LUAD, LUSC, PAAD, and THCA (*p*-values: 4.6×10^{-3}, 4.0×10^{-2}, 3.8×10^{-2}, 4.3×10^{-2}, 3.9×10^{-2}, 4.7×10^{-2}, and 3.6×10^{-2}, respectively; data not shown). The TPM level of *VIM* expression was higher for females in BRCA, GBM, LUAD, LUSC, and PAAD. In KIRC and THCA, expression of *VIM* was significantly elevated in the male subgroup (data not shown). We also investigate the correlation between *VIM* expression and individual cancer stages in groups where VIM expression has been elevated (data not shown). Our analysis confirms that in CHOL, HNSC, KIRC, KIRP, and LIHC the *VIM* expression has been statistically increased at every cancer stage (Stage from 1 to 4) in comparison to normal tissues (with one exception in stage 3 of CHOL, where was the only one sample). For GBM and PCPG, there was no available information in the database about *VIM* expression at individual cancer stages.

Figure 3. Expression and promoter methylation levels of *VIM* in primary tumor samples in comparison to healthy tissues according to data deposited in TCGA. (**A**) Expression of *VIM* in CHOL; (**B**) promoter methylation of *VIM* in CHOL; (**C**) expression of *VIM* in GBM; (**D**) promoter methylation of *VIM* in GBM; (**E**) expression of *VIM* in HNSC; (**F**) promoter methylation of *VIM* in HNSC; (**G**) expression of *VIM* in KIRC; (**H**) promoter methylation of *VIM* in KIRC. NS—not statistically significant; * $p \leq 0.05$, ** $p \leq 0.01$, and *** $p \leq 0.001$.

An analysis of the correlation of *VIM* expression with gene promoter methylation showed that, among all cancers for which the expression of *VIM* gene was significantly lower in cancer tissue than in normal tissue samples, the gene promoter methylation level was significantly higher ($p \leq 0.05$) in cancer tissue than in normal tissue in the cases of BLCA, BRCA, COAD, and LUSC (Table 2). However, we only observed a methylation difference ($\Delta\beta$-value = 0.10) for BRCA between normal and cancer tissue at a level that may indicate a biologically significant correlation of *VIM* promoter methylation and gene expression. Furthermore, among all cancers for which we observed overexpression of *VIM* gene in cancer tissues, the promoter methylation level was significantly lower ($p \leq 0.05$) in cancer tissues in the cases of KIRC and KIRP, with $\Delta\beta$-values of 0.14 and 0.07, respectively. These results revealed that lower *VIM* gene expression may be associated with a gain of gene promoter methylation in BRCA, whereas overexpression of *VIM* may be due to a loss of gene promoter methylation in KIRC and KIRP.

Table 2

Promoter methylation level of *VIM* in normal and primary tumor tissues according to data deposited in TCGA database. A *p*-value ≤ 0.05 was considered statistically significant (bolded in table). The Δβ-value indicates differences in the promoter methylation level of *VIM* between normal and primary tumor tissue.

	Values of *VIM* promoter methylation level in normal tissue				Values of *VIM* promoter methylation level in primary tumor tissue					
Tumor type	Number of samples	Minimal value	Median	Maximal Value	Number of samples	Minimal value	Median	Maximal value	Δβ-value	p-Value
BLCA	21	0.11	0.13	0.17	418	0.05	0.17	0.49	0. 05	**1.624478×10^{-12}**
BRCA	97	0.12	0.21	0.32	793	0.05	0.30	0.72	0.10	**$< 1 \times 10^{-12}$**
CHOL	9	0.22	0.25	0.32	36	0.09	0.32	0.83	0.07	**1.21594×10^{-2}**
COAD	37	0.08	0.13	0.19	313	0.06	0.15	0.31	0.02	**2.4513×10^{-10}**
ESCA	16	0.08	0.19	0.29	185	0.05	0.17	0.45	−0.03	5.9306×10^{-1}
GBM	2	0.23	0.24	0.25	140	0.07	0.16	0.32	−0.08	6.3986×10^{-1}
HNSC	50	0.11	0.16	0.23	528	0.06	0.16	0.40	−0.01	1.55862×10^{-1}
KIRC	160	0.19	0.26	0.34	324	0.07	0.12	0.22	−0.14	**1.624367×10^{-12}**
KIRP	45	0.20	0.25	0.29	275	0.05	0.18	0.45	−0.07	**1.0171×10^{-7}**
LIHC	50	0.18	0.25	0.35	377	0.05	0.21	0.60	−0.04	5.2152×10^{-1}
LUAD	32	0.14	0.18	0.23	473	0.08	0.17	0.32	−0.01	6.5876×10^{-2}
LUSC	42	0.09	0.13	0.16	370	0.06	0.13	0.31	0.00	**2.1553×10^{-8}**
PAAD	10	0.13	0.19	0.19	184	0.12	0.21	0.37	0.02	**1.7267×10^{-7}**
PCPG	3	0.14	0.15	0.16	179	0.09	0.26	0.69	0.11	**1.624589×10^{-12}**
READ	7	0.17	0.17	0.18	98	0.07	0.13	0.24	−0.04	**4.5475×10^{-2}**
SARC	4	0.08	0.09	0.11	261	0.06	0.13	0.28	0.04	**5.9909×10^{-4}**
STAD	2	0.16	0.19	0.21	395	0.06	0.2	0.54	0.01	5.4752×10^{-1}
THCA	56	0.15	0.21	0.29	507	0.06	0.19	0.38	−0.02	3.081×10^{-1}
THYM	2	0.12	0.17	0.22	124	0.07	0.19	0.39	0.02	4.2316×10^{-1}

BLCA—bladder urothelial carcinoma; BRCA—breast invasive carcinoma; CHOL—cholangiocarcinoma; COAD—colon adenocarcinoma; ESCA—esophageal carcinoma; GBM—glioblastoma multiforme; HNSC—head-and-neck squamous cell carcinoma; KIRC—kidney renal clear cell carcinoma; KIRP—kidney renal papillary cell carcinoma; LIHC—liver hepatocellular carcinoma; LUAD—lung adenocarcinoma; LUSC—lung squamous cell carcinoma; PAAD—pancreatic adenocarcinoma; PCPG—pheochromocytoma and paraganglioma; READ—rectum adenocarcinoma; SARC—sarcoma; STAD—stomach adenocarcinoma; THCA—thyroid carcinoma; THYM—thymoma.

3.2. Gene, Protein Interaction Network and Mutation Analysis of VIM

The protein–protein interaction network showed an association between genes for *VIM*. The GeneMANIA analysis revealed information about predicted gene functions using web analysis tool (Fig. 6A). The central node representing VIM was surrounded by 20 nodes representing genes that greatly correlated with VIM in terms of physical interaction, co-expression, predictions, co-localization, and genetic interactions. The genes displaying the strongest correlations with VIM included DES, TCAP, TTN, NEB, TMOD1 and SERPINH1. Further analysis, by the STRING database identified known interactions for 10 discovered proteins (Fig. 6B). *VIM* as the center node was associated with apoptotic proteins (caspase-3, -6, -7, and – 8), a transcription factor (signal transducer and activator of transcription 3 (STAT3)), and the muscle-specific IF desmin (DES). Thus, these protein partners predicted to interact with VIM might be involved in regulating cancer progression and prognosis. Analysis of the frequency of *VIM* mutations in different cancer types was performed using the cBioPortal database (Fig. 6C). Alterations were found in BLCA (4.87%) and endometrial carcinoma (4.44%), whereas renal carcinoma exhibited the lowest frequency (0.57%). Endometrial carcinoma presented the most mutations (3.24%), in contrast to diffuse glioma, which had the lowest number of mutations (0.19%). Ovarian epithelial tumor showed the highest amplification (2.91%), whereas the lowest value was discovered for non-small-cell lung cancer and HNSC (0.19% for both). In nonseminomatous germ cell tumor, alterations appeared only in the form of a deep deletion (1.16%). Interestingly, in adrenocortical carcinoma, we observed an equal frequency of mutations and deep deletions (1.1% for both).

4. Discussion

One of the main molecular mechanisms involved in oncogenesis and the promotion of cancer progression is epithelial-to-mesenchymal transition (EMT) (Meng 2011). During the EMT process, cells lose their epithelial characteristics, especially polarity, and obtain a migratory behavior (Xu 2009). This leads to them altering their shape and exhibiting increased motility (Xu 2009). Besides, persistent inflammation and hypoxia lead to creating a specific micro-environment in which the interaction between normal and neoplastic cells (like direct contact, secretion of active substances) contributes to a change in the tumor phenotype during EMT (Huber 2005; Hugo 2007; Qureshi 2015). The EMT process is widely described in the literature and plays an essential role in the stages of cancer development. First, cells acquire the ability to migrate, which means that they can separate themselves from the rest of the population. Second, the transition process allows cells to access regional lymph nodes as well as blood vessels; thirdly, it enables the continuous leaving of the original site and the creation of micro-metastases (Huber 2005; Hugo 2007; Qureshi 2015). The acquired mesenchymal phenotype is connected with the expression of mesenchymal cytoskeletal proteins, such as vimentin, which induces the formation of focal adhesion complexes, thereby facilitating cell migration (Imamichi and Menke 2007; Zhao 2009).

In recent years, there has been growing interest in the biological function of vimentin (Menko 2014; Cheng 2016; Ghosh 2018; Patteson 2019; Li and Kuemmerle 2020; Li 2020; Zhang 2020; Suprewicz 2021). As a multifunctional protein, vimentin is differentially expressed in diverse cell types, whereby it may also play a tissue-specific function. Study on knockout mice ($vim^{-/-}$) showed that a lack of vimentin or destabilization of the vimentin network enhances lamellipodia formation in all directions without net cell displacement (Helfand 2011). Cancer is one of the most common causes of death worldwide (Siegel 2021). It is estimated that, in the last year, this problem increased worldwide, mainly due to the limited access to diagnostics and appropriate therapies resulting from the ongoing pandemic. In this work, we analyzed the expression of *VIM* as a potential biomarker and a therapeutic target in diverse cancers.

The result of our study showed that, out of 33 available records, only 19 types of cancer contained complete information about *VIM* expression, gender, and promoter methylation in TCGA. Overexpression of *VIM* was detected for seven cancers, namely, CHOL, GBM, HNSC, KIRC, KIRP, LIHC, and PCPG. Moreover, the increased *VIM* expression has been proved in every stage of the disease for CHOL, HNSC, KIRC, KIRP, and LIHC. Decreased expression of *VIM* was reported for six types of cancers, namely, BLCA, BRCA, COAD, LUAD, LUSC, and READ. For the others, six cases of nonstatistical significances were observed where *VIM* expression was distinct (ESCA, PAAD, SARC, STAD, THYM, and THCA). Studies also showed that the overexpression of *VIM* was mostly higher among females. The analysis of correlation between *VIM* expression and gene promoter methylation showed that, among all defined cancers with a significant difference in gene expression level, the expression of *VIM* may be regulated by promoter methylation in the cases of KIRC, KIRP, and BRCA. The analysis of protein–protein interactions using GeneMANIA and STRING leads us to suspect that these protein partners predicted to interact with *VIM* might be involved in the regulation of *VIM*-mediated cancer progression and prognosis.

We are aware that our research may have some limitation. The first is the inconsiderable number of patients, especially in normal tissue samples in CHOL, ESCA, GBM, PAAD, PCPG, and THYM. Given that in some cases our findings are based on a limited number of data, the result from such analyses should therefore be treated with caution. This finding needs to be confirmed on a larger group of patients. The second limitation is the lack of own analyses that could confirm or contradict conclusions drawn only from bioinformatic analyses. The third is that extracellular *VIM* expression was not determined in this study. These limitations highlight the difficulties that must be considered while conducting the bioinformatic analysis. Further data collection is required to determinate precisely the role of *VIM* as a potential diagnostic biomarker. In addition, it should be emphasized that the human body is a combination of different types of cells. Even within one organ, we often observe many different types of cells with different biological functions. For example, the liver tissue is a combination of hepatocytes, cholangiocytes, sinusoidal endothelial cells, Kupffer cells and hepatic stellate cells (Puche 2013). Thus, the precise determination of *VIM* expression in each cell group may provide the basis for a better understanding of its biological function.

The overexpression of *VIM* seen in numerous cancer studies indicates that gene expression may be directly related to a specific cancer's aggressiveness (e.g., hepatocellular carcinoma and stomach adenocarcinoma). However, in both of these cancer types, different mechanisms underlying vimentin's contribution were observed (Takemura 1994; Fuyuhiro 2010). In stomach cancer, *VIM* overexpression is correlated with a significantly higher incidence of lymph-node metastasis (Jin 2010). In contrast to previous data, overexpression of *VIM* in LIHC cells suppresses their proliferative and invasive capabilities (Li 2008). Moreover, the enhanced expression of *VIM* in colorectal cancer is positively correlated with expanded migration and invasive potential (McInroy and Maatta 2007). Despite the more effective diagnosis of gastric cancers, their mortality rate remains high, with a < 30% survival rate (Zhu 2017). Furthermore, elevated *VIM* expression has been reported in lung cancer (Helfand 2011), and it is also a prognostic factor of poor survival in non-small-cell lung cancer (Richardson 2012). Moreover, *VIM* overexpression in breast cancers is correlated with increased invasion and promotes epithelial cell migration (Gilles 1999; Kokkinos 2007). Silencing of *VIM* in cisplatin-resistant ovarian cancer cell lines A2780-DR and HO-8910 increased the expression levels of exocytotic proteins, which have been proposed as a new therapeutic target for treating drug-resistant ovarian cancer (Huo 2016).

VIM expression can be modulated at the transcriptional level by noncoding RNA, especially microRNA (miRNA). These small molecules, the expression levels of which are disrupted in cancer, could impact target genes. Additionally, *VIM* is directly or indirectly targeted by miRNA, making it a potential target in therapies. It has been proven that, in breast cancer cells, miR-138 modulates metastasis and EMT (Zhang 2016). Another molecule, miR-122, may affect tissue-remodeling genes, such as *VIM* or hypoxia-inducible factor-1 (HIF-1α), potentially inducing endothelial–mesenchymal transition (Csak 2015). Furthermore, miR-141 and miR-200c regulate vimentin by suppressing its expression in renal tubular epithelial cells (Shi 2014; Huang 2015; Tanaka 2015). Moreover, in gastric cancers, overexpression of miR-1275 could indirectly repress the metastasis and invasion of cancer cells via *VIM* (Mei 2019). Furthermore, overexpression of miR-1246 inhibited the activities of vimentin and N-cadherin through inhibiting EMT in prostate cancer (Bhagirath 2018). Nevertheless, according to miRTarBase (http://mirtarbase.mbc.nctu.edu.tw/php/index.php), which is the starting point for many researchers, *VIM* is only a target gene for human miRNAs miR-9, -138, -30a, -26b, -17, -16, -1301, -615, -3605, -378a, and − 506. The discovery of miRNAs has offered great hope for the diagnosis, prognosis, and potential prediction of many diseases, including cancers.

Recent studies also showed that vimentin could play a crucial role in cancer development and subsequent reaction of the immune system. Researchers suggest that vimentin is involved in the apoptosis of neutrophils and lymphocytes (Morishima 1999; Byun 2001; Lavastre 2002; Moisan and Girard 2006; Hsu 2014). Interestingly, Su et al. (Su 2019) also reported a positive role of vimentin in lymphocyte apoptosis, which may serve as a potential serum biomarker for sepsis prognosis. Moreover, vimentin has also been proposed as a possible cellular target for the treatment of coronavirus disease 19 (COVID-19) (Li 2020; Zhang 2020). Because vimentin is suggested as a co-receptor for the entry of SARS-CoV-2 into cells, drugs that decrease the expression of vimentin can be used to treat patients with COVID-19 (Yu 2016).

On one hand, *VIM* could represent a good biomarker with diagnostic implications when it is overexpressed in specific cancer types. On the other hand, we assume that the decreased expression of *VIM* could potentially be key for therapeutic approaches. This study only used bioinformatics analyses available on online databases. Furthermore, investigations of vimentin during carcinogenesis are necessary to optimize experimental and clinical therapeutic approaches for cancer patients. Evaluation of the expression patterns of distinct genes in normal and cancer tissues may be of superior value in tumor diagnosis and prognosis. Since the spread of cancer

cells is considered to be one of the most important causes of disease progression, treatment failure, and consequently patient death, identifying markers which allow rapid detection of this process can be a breakthrough in cancer treatment. A comprehensive approach which takes into consideration the interactions between molecular profiles and the metastasis of cancer cells might also allow for the development of personalized therapy. Lastly, using the databases highlighted in this study, researchers could explore additional signaling networks in cancer or other diseases, including viral infections.

5. Conclusions

In the current study, we used several online bioinformatics platforms and web tools (TCGA UALCAN, GeneMANIA, STRING, and cBioPortal) to conduct a systematic analysis of *VIM* expression in selected types of cancer. We proved that *VIM* is overexpressed in CHOL, GBM, HNSC, and KIRC, especially among women. The analysis of correlation between *VIM* expression and gene promoter methylation demonstrated that *VIM* expression may be regulated by promoter methylation in three types of cancer (KIRC, KIRP, and BRCA). Our analysis suggests that *VIM* overexpression may be a potentially novel diagnostic biomarker in selected cancers. Moreover, *VIM* could be a potential therapeutic target for a further analysis.

Abbreviations

AKT1—RAC-alpha serine/threonine protein kinase

BLCA—Bladder urothelial carcinoma

BRCA—Breast invasive carcinoma

CASP3—Caspase-3

CASP6—Caspase-6

CASP7—Caspase-7

CASP8—Caspase-8

CDC5L—Cell division cycle 5-like protein

CESC—Cervical squamous cell carcinoma

CHOL—Cholangiocarcinoma

COAD—Colon adenocarcinoma

COVID-19—Coronavirus disease 2019

DES—Desmin

ESCA—Esophageal carcinoma

EMT—Epithelial-to-mesenchymal transition

GBM—Glioblastoma multiforme

HIF-1α—Hypoxia-inducible factor-1

HIV—Human immunodeficiency virus

HNSC—Head-and-neck squamous cell carcinoma

IF—Intermediate filament

KICH—Kidney chromophobe

KIRC—Kidney renal clear cell carcinoma

KIRP—Kidney renal papillary cell carcinoma

LIHC—Liver hepatocellular carcinoma

LPS—Lipopolysaccharides

LUAD—Lung adenocarcinoma

LUSC—Lung squamous cell carcinoma

miRNA—MicroRNA

NS—Not statistically significant

PAAD—Pancreatic adenocarcinoma

PRAD—Prostate adenocarcinoma

PCPG—Pheochromocytoma and paraganglioma

READ—Rectum adenocarcinoma

SARC—Sarcoma

SARS-CoV-2—Severe acute respiratory syndrome coronavirus 2

SKCM—Skin cutaneous melanoma

STAD—Stomach adenocarcinoma

STAT3—Signal transducer and activator of transcription 3

TCGA—The Cancer Genome Atlas

THCA—Thyroid carcinoma

THYM—Thymoma

TPM—Transcripts per million

TPM2—Tropomyosin beta chain

TPM4—Tropomyosin alpha-4 chain

VIM—Vimentin

USC—Uterine carcinosarcoma

Declarations

Author Contributions: Conceptualization, M.B. and B.H.-Sz.; methodology, M.B., P.B., O.T.-L., and B.H.-Sz.; software, M.B.; formal analysis, M.B., P.B., O.T.-L., and B.H.-Sz.; investigation, M.B.; resources, M.B.; data curation, M.B.; writing—original draft preparation, M.B., P.B., O.T.-L., and B.H.-Sz.; writing—review and editing, M.B. and B.H.-Sz.; visualization, M.B.; supervision, M.B., P.B., O.T.-L., and B.H.-Sz.; project administration, M.B. All authors read and agreed to the published version of the manuscript.

Funding: This research received no external funding.

Conflicts of Interest: The authors declare no conflicts of interest.

References

Bhagirath, D., et al. (2018). microRNA-1246 Is an Exosomal Biomarker for Aggressive Prostate Cancer. Cancer Res 78(7): 1833-1844 10.1158/0008-5472.CAN-17-2069

Byun, Y., et al. (2001). Caspase cleavage of vimentin disrupts intermediate filaments and promotes apoptosis. Cell Death Differ 8(5): 443-450 10.1038/sj.cdd.4400840

Cain, H., et al. (1983). Vimentin filaments in peritoneal macrophages at various stages of differentiation and with altered function. Virchows Arch B Cell Pathol Incl Mol Pathol 42(1): 65-81 10.1007/BF02890371

Chandrashekar, D. S., et al. (2017). UALCAN: A Portal for Facilitating Tumor Subgroup Gene Expression and Survival Analyses. Neoplasia 19(8): 649-658 10.1016/j.neo.2017.05.002

Cheng, F., et al. (2016). Vimentin coordinates fibroblast proliferation and keratinocyte differentiation in wound healing via TGF-beta-Slug signaling. Proc Natl Acad Sci U S A 113(30): E4320-4327 10.1073/pnas.1519197113

Cong, H., et al. (2016). DNA hypermethylation of the vimentin gene inversely correlates with vimentin expression in intestinal- and diffuse-type gastric cancer. Oncol Lett 11(1): 842-848 10.3892/ol.2015.3937

Csak, T., et al. (2015). microRNA-122 regulates hypoxia-inducible factor-1 and vimentin in hepatocytes and correlates with fibrosis in diet-induced steatohepatitis. Liver Int 35(2): 532-541 10.1111/liv.12633

Eckes, B., et al. (1998). Impaired mechanical stability, migration and contractile capacity in vimentin-deficient fibroblasts. J Cell Sci 111 (Pt 13): 1897-1907

Eriksson, J. E., et al. (2009). Introducing intermediate filaments: from discovery to disease. J Clin Invest 119(7): 1763-1771 10.1172/JCI38339

Fernandez-Ortega, C., et al. (2016). Identification of Vimentin as a Potential Therapeutic Target against HIV Infection. Viruses 8(6) 10.3390/v8060098

Franke, W. W., et al. (1978). Different intermediate-sized filaments distinguished by immunofluorescence microscopy. Proc Natl Acad Sci U S A 75(10): 5034-5038 10.1073/pnas.75.10.5034

Fuyuhiro, Y., et al. (2010). Clinical significance of vimentin-positive gastric cancer cells. Anticancer Res 30(12): 5239-5243

Gao, J., et al. (2013). Integrative analysis of complex cancer genomics and clinical profiles using the cBioPortal. Sci Signal 6(269): pl1 10.1126/scisignal.2004088

Ghosh, P., et al. (2018). Invasion of the Brain by Listeria monocytogenes Is Mediated by InlF and Host Cell Vimentin. mBio 9(1) 10.1128/mBio.00160-18

Gilles, C., et al. (1999). Vimentin contributes to human mammary epithelial cell migration. J Cell Sci 112 (Pt 24): 4615-4625

Helfand, B. T., et al. (2011). Vimentin organization modulates the formation of lamellipodia. Mol Biol Cell 22(8): 1274-1289 10.1091/mbc.E10-08-0699

Hsu, P. C., et al. (2014). Vimentin is involved in peptidylarginine deiminase 2-induced apoptosis of activated Jurkat cells. Mol Cells 37(5): 426-434 10.14348/molcells.2014.2359

Huang, Y., et al. (2015). miR-141 regulates TGF-beta1-induced epithelial-mesenchymal transition through repression of HIPK2 expression in renal tubular epithelial cells. Int J Mol Med 35(2): 311-318 10.3892/ijmm.2014.2008

Huber, M. A., et al. (2005). Molecular requirements for epithelial-mesenchymal transition during tumor progression. Curr Opin Cell Biol 17(5): 548-558 10.1016/j.ceb.2005.08.001

Hugo, H., et al. (2007). Epithelial--mesenchymal and mesenchymal--epithelial transitions in carcinoma progression. J Cell Physiol 213(2): 374-383 10.1002/jcp.21223

Huo, Y., et al. (2016). Downregulation of vimentin expression increased drug resistance in ovarian cancer cells. Oncotarget 7(29): 45876-45888 10.18632/oncotarget.9970

Imamichi, Y. and A. Menke (2007). Signaling pathways involved in collagen-induced disruption of the E-cadherin complex during epithelial-mesenchymal transition. Cells Tissues Organs 185(1-3): 180-190 10.1159/000101319

Jin, H., et al. (2010). Vimentin expression of esophageal squamous cell carcinoma and its aggressive potential for lymph node metastasis. Biomed Res 31(2): 105-112 10.2220/biomedres.31.105

Kokkinos, M. I., et al. (2007). Vimentin and epithelial-mesenchymal transition in human breast cancer--observations in vitro and in vivo. Cells Tissues Organs 185(1-3): 191-203 10.1159/000101320

Lavastre, V., et al. (2002). Mechanisms involved in spontaneous and Viscum album agglutinin-I-induced human neutrophil apoptosis: Viscum album agglutinin-I accelerates the loss of antiapoptotic Mcl-1 expression and the degradation of cytoskeletal paxillin and vimentin proteins via caspases. J Immunol 168(3): 1419-1427 10.4049/jimmunol.168.3.1419

Lee, S. J., et al. (2014). The expression and secretion of vimentin in the progression of non-alcoholic steatohepatitis. BMB Rep 47(8): 457-462 10.5483/bmbrep.2014.47.8.256

Li, C. and J. F. Kuemmerle (2020). The fate of myofibroblasts during the development of fibrosis in Crohn's disease. J Dig Dis 21(6): 326-331 10.1111/1751-2980.12852

Li, K., et al. (2018). Identification of gene-specific DNA methylation signature for Colorectal Cancer. Cancer Genet 228-229: 5-11 10.1016/j.cancergen.2018.05.003

Li, Z., et al. (2020). Vimentin as a target for the treatment of COVID-19. BMJ Open Respir Res 7(1) 10.1136/bmjresp-2020-000623

Li, Z. M., et al. (2008). [Enhanced expression of human vimentin intermediate filaments in hepatocellular carcinoma cells decreases their proliferative and invasive abilities in vitro]. Zhonghua Zhong Liu Za Zhi 30(6): 408-412

Loberg, R. D., et al. (2005). Pathogenesis and treatment of prostate cancer bone metastases: targeting the lethal phenotype. J Clin Oncol 23(32): 8232-8241 10.1200/JCO.2005.03.0841

Lowery, J., et al. (2015). Intermediate Filaments Play a Pivotal Role in Regulating Cell Architecture and Function. J Biol Chem 290(28): 17145-17153 10.1074/jbc.R115.640359

McInroy, L. and A. Maatta (2007). Down-regulation of vimentin expression inhibits carcinoma cell migration and adhesion. Biochem Biophys Res Commun 360(1): 109-114 10.1016/j.bbrc.2007.06.036

Mei, J. W., et al. (2019). MicroRNA-1275 inhibits cell migration and invasion in gastric cancer by regulating vimentin and E-cadherin via JAZF1. BMC Cancer 19(1): 740 10.1186/s12885-019-5929-1

Meng, X., et al. (2011). Requirement of podocalyxin in TGF-beta induced epithelial mesenchymal transition. PLoS One 6(4): e18715 10.1371/journal.pone.0018715

Menko, A. S., et al. (2014). A central role for vimentin in regulating repair function during healing of the lens epithelium. Mol Biol Cell 25(6): 776-790 10.1091/mbc.E12-12-0900

Moisan, E. and D. Girard (2006). Cell surface expression of intermediate filament proteins vimentin and lamin B1 in human neutrophil spontaneous apoptosis. J Leukoc Biol 79(3): 489-498 10.1189/jlb.0405190

Morishima, N. (1999). Changes in nuclear morphology during apoptosis correlate with vimentin cleavage by different caspases located either upstream or downstream of Bcl-2 action. Genes Cells 4(7): 401-414 10.1046/j.1365-2443.1999.00270.x

Patteson, A. E., et al. (2019). Loss of Vimentin Enhances Cell Motility through Small Confining Spaces. Small 15(50): e1903180 10.1002/smll.201903180

Perreau, J., et al. (1988). Nucleotide sequence of the human vimentin gene and regulation of its transcription in tissues and cultured cells. Gene 62(1): 7-16 10.1016/0378-1119(88)90575-6

Puche, J. E., et al. (2013). Hepatic stellate cells and liver fibrosis. Compr Physiol 3(4): 1473-1492 10.1002/cphy.c120035

Qureshi, R., et al. (2015). EMT in cervical cancer: its role in tumour progression and response to therapy. Cancer Lett 356(2 Pt B): 321-331 10.1016/j.canlet.2014.09.021

Rathje, L. S., et al. (2014). Oncogenes induce a vimentin filament collapse mediated by HDAC6 that is linked to cell stiffness. Proc Natl Acad Sci U S A 111(4): 1515-1520 10.1073/pnas.1300238111

Richardson, F., et al. (2012). The evaluation of E-Cadherin and vimentin as biomarkers of clinical outcomes among patients with non-small cell lung cancer treated with erlotinib as second- or third-line therapy. Anticancer Res 32(2): 537-552

Rittling, S. R. and R. Baserga (1987). Functional analysis and growth factor regulation of the human vimentin promoter. Mol Cell Biol 7(11): 3908-3915 10.1128/mcb.7.11.3908

Shi, R., et al. (2014). Effects of miR-200c on the migration and invasion abilities of human prostate cancer Du145 cells and the corresponding mechanism. Front Med 8(4): 456-463 10.1007/s11684-014-0353-z

Siegel, R. L., et al. (2021). Cancer Statistics, 2021. CA Cancer J Clin 71(1): 7-33 10.3322/caac.21654

Sommers, C. L., et al. (1989). Vimentin rather than keratin expression in some hormone-independent breast cancer cell lines and in oncogene-transformed mammary epithelial cells. Cancer Res 49(15): 4258-4263

Su, L., et al. (2019). Role of vimentin in modulating immune cell apoptosis and inflammatory responses in sepsis. Sci Rep 9(1): 5747 10.1038/s41598-019-42287-7

Suprewicz, L., et al. (2021). Vimentin binds to SARS-CoV-2 spike protein and antibodies targeting extracellular vimentin block in vitro uptake of SARS-CoV-2 virus-like particles. bioRxiv 10.1101/2021.01.08.425793

Szklarczyk, D., et al. (2019). STRING v11: protein-protein association networks with increased coverage, supporting functional discovery in genome-wide experimental datasets. Nucleic Acids Res 47(D1): D607-D613 10.1093/nar/gky1131

Takemura, K., et al. (1994). Expression of vimentin in gastric cancer: a possible indicator for prognosis. Pathobiology 62(3): 149-154 10.1159/000163895

Tanaka, S., et al. (2015). Induction of epithelial-mesenchymal transition and down-regulation of miR-200c and miR-141 in oxaliplatin-resistant colorectal cancer cells. Biol Pharm Bull 38(3): 435-440 10.1248/bpb.b14-00695

Uhlen, M., et al. (2015). Proteomics. Tissue-based map of the human proteome. Science 347(6220): 1260419 10.1126/science.1260419

Ulirsch, J., et al. (2013). Vimentin DNA methylation predicts survival in breast cancer. Breast Cancer Res Treat 137(2): 383-396 10.1007/s10549-012-2353-5

Warde-Farley, D., et al. (2010). The GeneMANIA prediction server: biological network integration for gene prioritization and predicting gene function. Nucleic Acids Res 38(Web Server issue): W214-220 10.1093/nar/gkq537

Xu, J., et al. (2009). TGF-beta-induced epithelial to mesenchymal transition. Cell Res 19(2): 156-172 10.1038/cr.2009.5

Yu, M. B., et al. (2018). Extracellular vimentin modulates human dendritic cell activation. Mol Immunol 104: 37-46 10.1016/j.molimm.2018.09.017

Yu, Y. T., et al. (2016). Surface vimentin is critical for the cell entry of SARS-CoV. J Biomed Sci 23: 14 10.1186/s12929-016-0234-7

Zhang, J., et al. (2016). MicroRNA-138 modulates metastasis and EMT in breast cancer cells by targeting vimentin. Biomed Pharmacother 77: 135-141 10.1016/j.biopha.2015.12.018

Zhang, Y., et al. (2020). The diverse roles and dynamic rearrangement of vimentin during viral infection. J Cell Sci 134(5) 10.1242/jcs.250597

Zhao, Y., et al. (2009). The lysyl oxidase pro-peptide attenuates fibronectin-mediated activation of focal adhesion kinase and p130Cas in breast cancer cells. J Biol Chem 284(3): 1385-1393 10.1074/jbc.M802612200

Zhou, T., et al. (2019). Knockdown of vimentin reduces mesenchymal phenotype of cholangiocytes in the Mdr2(-/-) mouse model of primary sclerosing cholangitis (PSC). EBioMedicine 48: 130-142 10.1016/j.ebiom.2019.09.013

Zhu, Y., et al. (2017). USP14 de-ubiquitinates vimentin and miR-320a modulates USP14 and vimentin to contribute to malignancy in gastric cancer cells. Oncotarget 8(30): 48725-48736 10.18632/oncotarget.10706

Zuberi, K., et al. (2013). GeneMANIA prediction server 2013 update. Nucleic Acids Res 41(Web Server issue): W115-122 10.1093/nar/gkt533

Figures

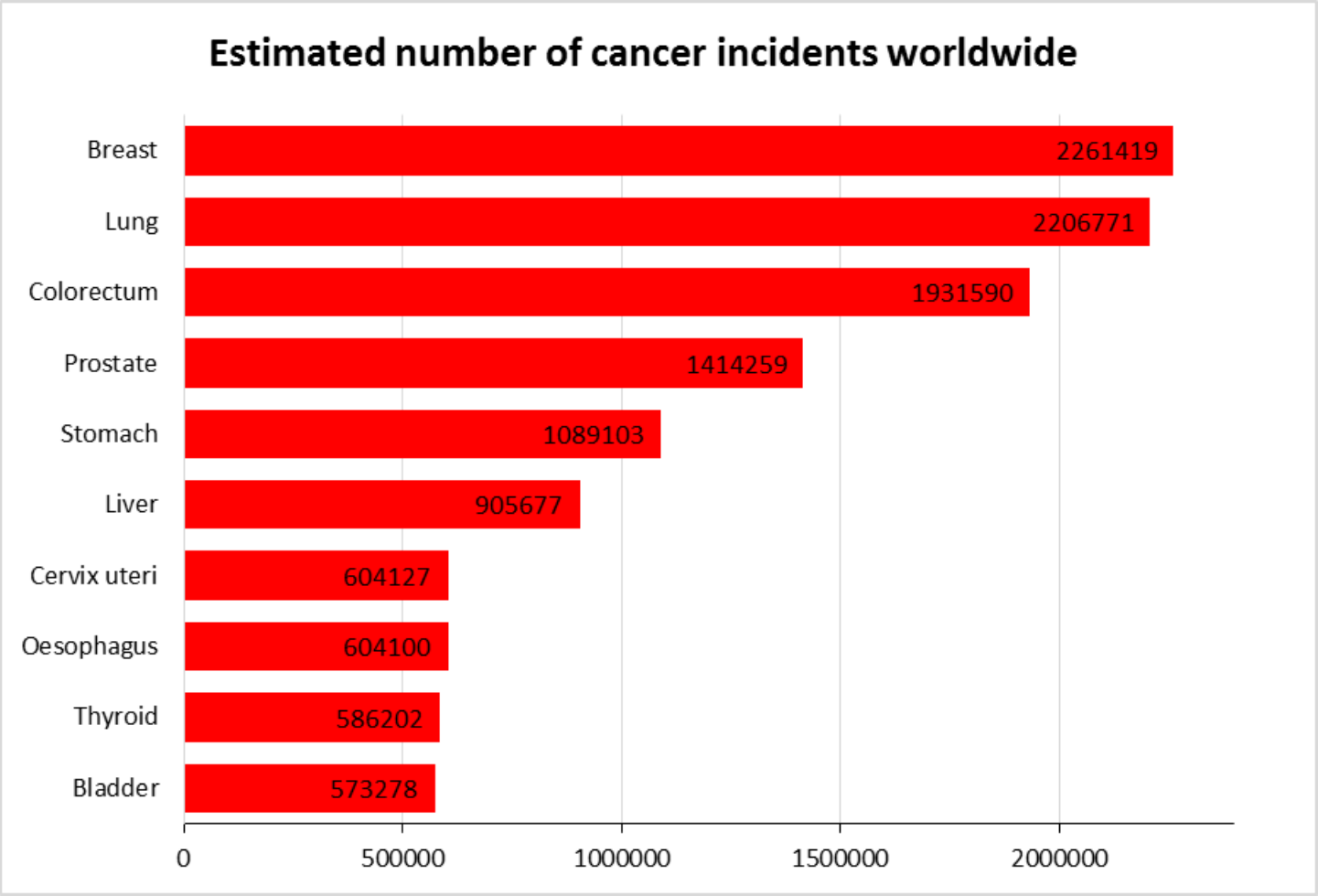

Figure 1

Global cancer incidence cases in 2020, worldwide, for both sexes and all ages, according to the Globocan data source by the World Health Organization.

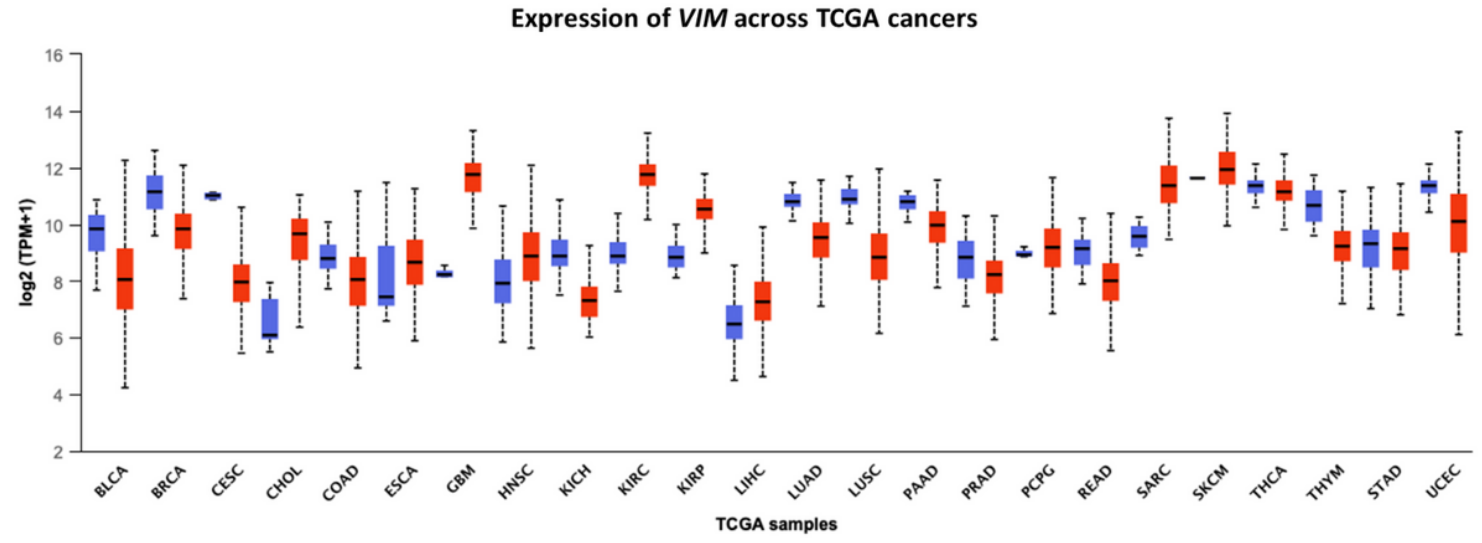

Figure 2

Expression level of vimentin gene (VIM) in normal and cancer tissues, according to The Cancer Genome Atlas (TCGA). Blue box plots depict normal tissue, whereas red box plots depict primary tumor samples. TPM—transcripts per million; BLCA—bladder

urothelial carcinoma; BRCA—breast invasive carcinoma; CESC—cervical squamous cell carcinoma; CHOL—cholangiocarcinoma; COAD—colon adenocarcinoma; ESCA—esophageal carcinoma; GBM—glioblastoma multi-forme; HNSC—head-and-neck squamous cell carcinoma; KICH—kidney chromophobe; KIRC—kidney renal clear cell carci-noma; KIRP—kidney renal papillary cell carcinoma; LIHC—liver hepatocellular carcinoma; LUAD—lung adenocarcinoma; LUSC—lung squamous cell carcinoma; PAAD—pancreatic adenocarcinoma; PRAD—prostate adenocarcinoma; PCPG—pheochromocytoma and paraganglioma; READ—rectum adenocarcinoma; SARC—sarcoma; SKCM—skin cutaneous melanoma; THCA—thyroid carcinoma; THYM—thymoma; STAD—stomach adenocarcinoma; UCEC— uterine corpus en-dometrial carcinoma.

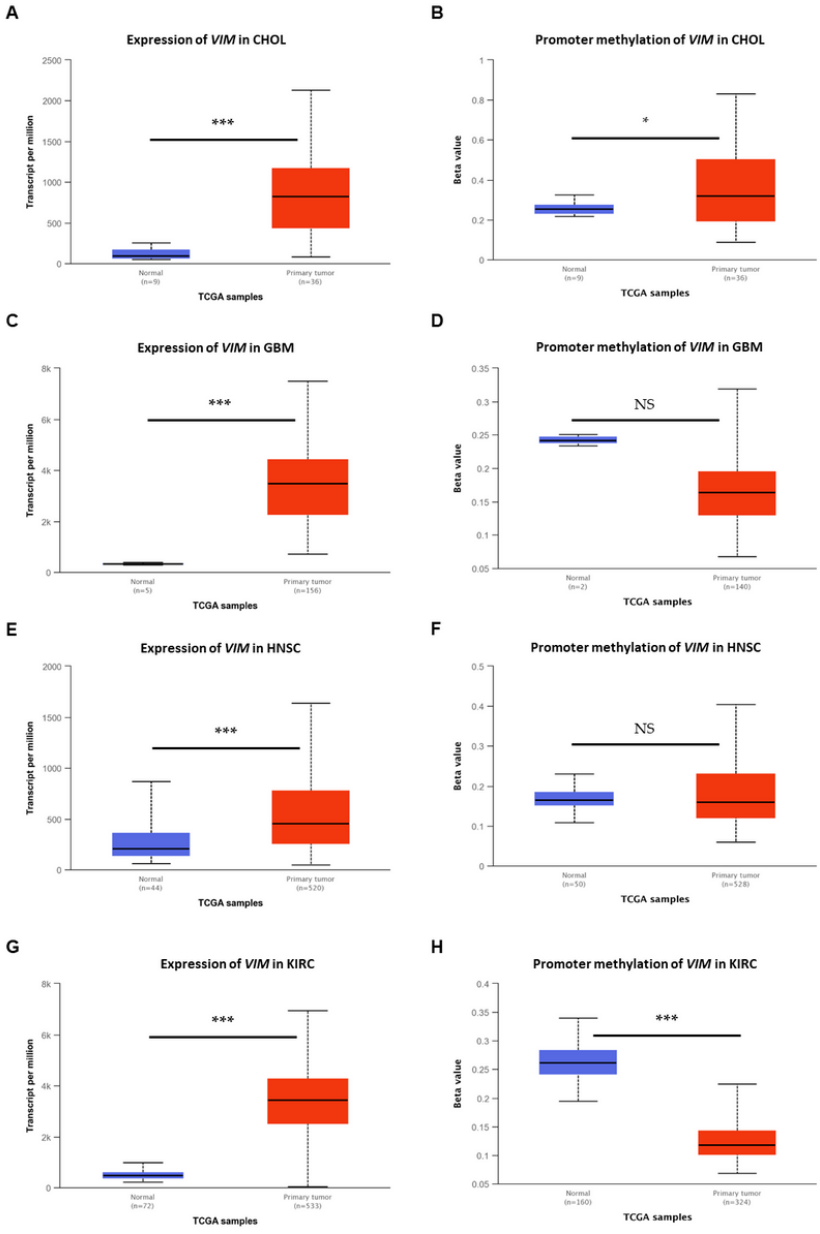

Figure 3

Expression and promoter methylation levels of VIM in primary tumor samples in comparison to healthy tissues according to data deposited in TCGA. (A) Expression of VIM in CHOL; (B) promoter methylation of VIM in CHOL; (C) expression of VIM in GBM; (D) promoter methylation of VIM in GBM; (E) expression of VIM in HNSC; (F) promoter methylation of VIM in HNSC; (G) ex-pression of VIM in KIRC; (H) promoter methylation of VIM in KIRC. NS—not statistically significant; * $p \leq 0.05$, ** $p \leq 0.01$, and *** $p \leq 0.001$.

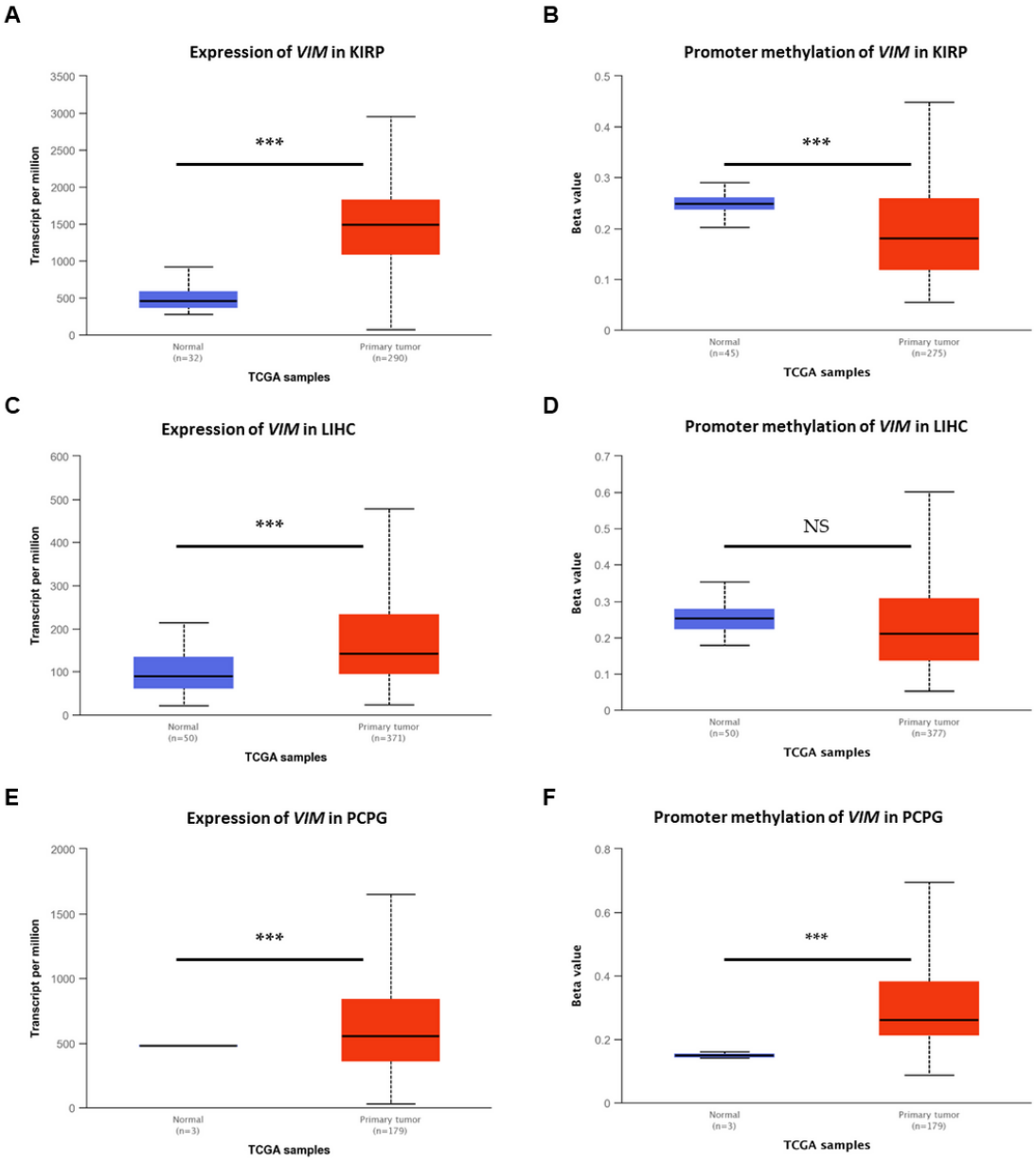

Figure 4

Expression and promoter methylation levels of VIM in primary tumor samples in comparison to healthy tissues according to data deposited in TCGA. (A) Expression of VIM in KIRP; (B) promoter methylation of VIM in KIRP; (C) expression of VIM in LIHC; (D) promoter methylation of VIM in LIHC; (E) expression of VIM in PCPG; (F) promoter methylation of VIM in PCPG. NS—not statistically significant; * $p \leq 0.05$, ** $p \leq 0.01$, and *** $p \leq 0.001$.

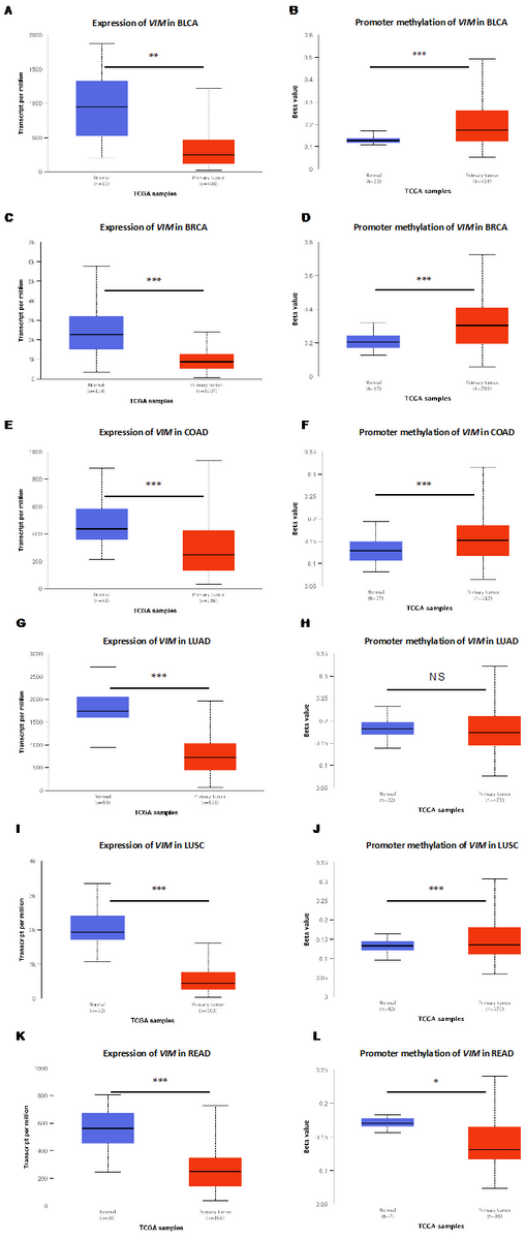

Figure 5

Expression and promoter methylation levels of VIM in primary tumor samples in comparison to healthy tissues according to data deposited in TCGA. (A) Expression of VIM in BLCA; (B) promoter methylation of VIM in BLCA; (C) expression of VIM in BRCA; (D) promoter methylation of VIM in BRCA; (E) expression of VIM in COAD; (F) promoter methylation of VIM in COAD; (G) Expression of VIM in LUAD; (H) promoter methylation of VIM in LUAD; (I) expression of VIM in LUSC; (J) promoter meth-ylation of VIM in LUSC; (K) expression of VIM in READ; (L) promoter methylation of VIM in READ. NS—not statistically sig-nificant; * $p \leq 0.05$, ** $p \leq 0.01$, and *** $p \leq 0.001$.

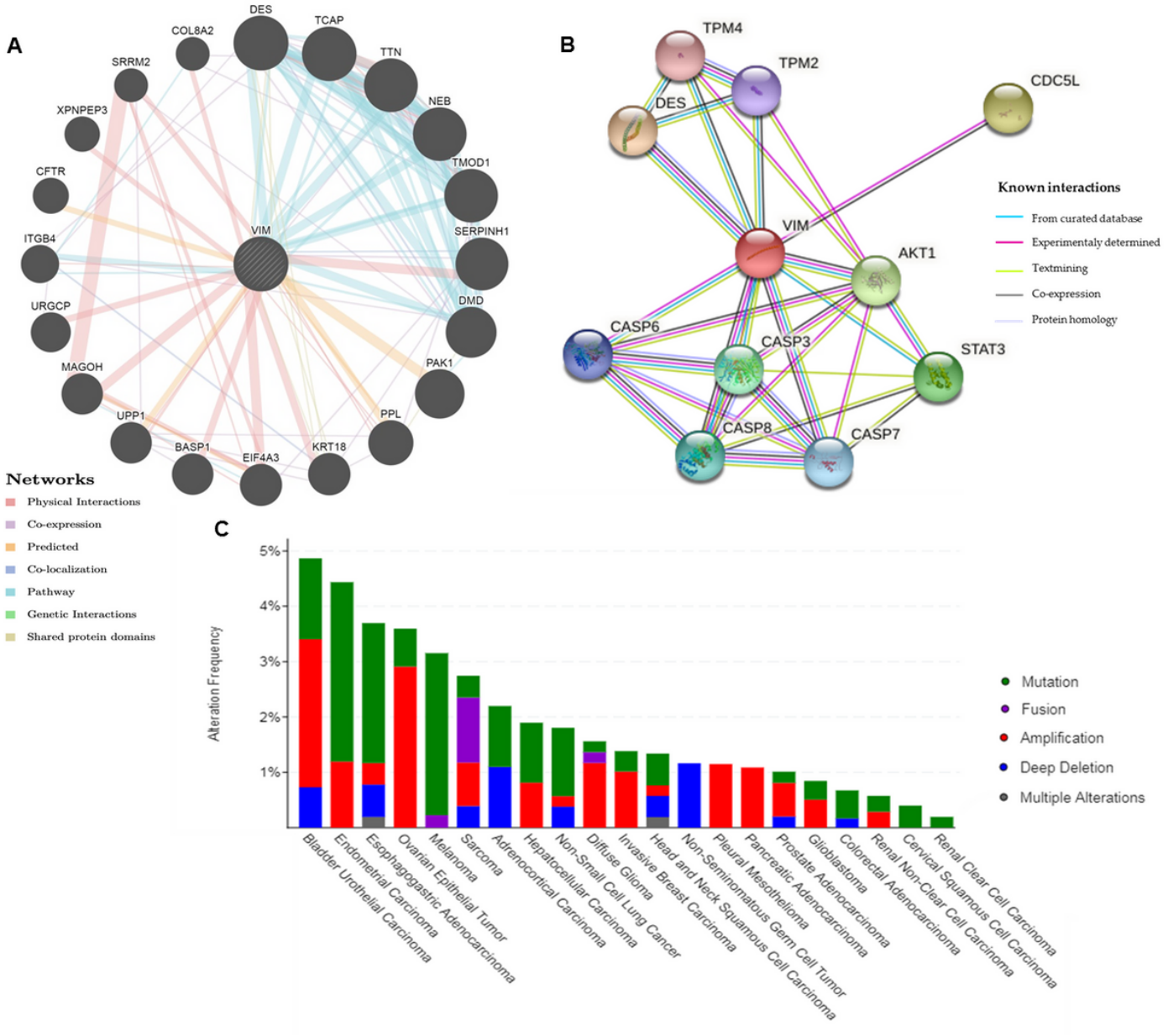

Figure 6

Protein–protein interaction network of vimentin. (A) GeneMANIA analysis with VIM placed at the center of diagram. The differ-ent colors of network edges indicate the bioinformatics methods applied: physical interaction, co-expression, prediction, co-localization, pathway, genetic interaction, and shared protein domains. (B) Search Tool for the Retrieval of Interacting Genes (STRING) analysis of VIM. Interacting nodes are displayed in colored circles. (C) Copy number alterations of VIM genes and cancer subtypes according to cBioPortal. All abbreviations are listed in the dedicated subsection at the end of the document.